Study of interference between surface plasmon polaritons by leakage radiation microscopy

Luis Grave de Peralta

Department of Physics and Nano Technology Center, Texas Tech University, Lubbock, Texas 79409, USA (luis.grave-de-peralta@ttu.edu)

Received April 29, 2010; accepted June 7, 2010;
posted June 10, 2010 (Doc. ID 127803); published July 9, 2010

Interference between two perpendicular surface plasmon polariton (SPP) beams was studied using a leakage radiation microscope, which allows for the observation of SPP propagation without disturbing the two-dimensional interference pattern formed at the region where the beams cross each other. Interference fringes were observed at the image plane of the microscope. Experimental results were discussed using both classical and quantum descriptions of light. Features observed in the Fourier-plane image directly demonstrate that, in correspondence with the widespread quantum description of light, photons do not propagate following the classical lines of electromagnetic energy flow. © 2010 Optical Society of America

OCIS codes: 240.6680, 000.2658, 070.7345, 110.0180.

1. INTRODUCTION

Leakage radiation microscopy (LRM) is a recently developed imaging technique that relies on the collection of light that leaks during surface plasmon polariton (SPP) propagation [1–4]. LRM provides raster free images along with the capability of Fourier-plane imaging [1–6]. In LRM the photons used for imaging are the ones that regardless of the measurement process leak to the sample substrate. This makes LRM an ideal technique to study interference between SPP beams because LRM allows for the observation of SPP propagation without disturbing the two-dimensional interference pattern formed at the region where beams cross each other. In this work, interference between two perpendicular SPP beams is studied using LRM techniques. The simple geometry of the experiments described here facilitates the theoretical discussion of the experimental results. The unique non-perturbing capabilities of LRM were used to conduct experiments that, in agreement with widespread quantum descriptions of light, demonstrate that photons do not propagate following the lines of electromagnetic energy flux [7,8]. This is not a trivial result. Since photons are quanta of electromagnetic energy, it has been argued that they should propagate following the classical lines of electromagnetic energy flow [9–12]. Even when this hypothesis is in contrast with the more intuitive picture of straight propagation of photons in free space, direct experimental evidence of straight propagation of photons during the superposition of two perpendicular beams of light is difficult to obtain experimentally. This is because the introduction of a photodetector in the beams' crossing region would result in the distortion of the original path of the photons. A similar hypothesis about the propagation of non-relativistic particles has been proposed. In the de Broglie–Bohm causal quantum mechanics [13–16], non-relativistic electrons propagate following "wiggling" trajectories that resemble the lines of energy flow in electrodynamics [15,16]. No experiment has been conducted to conclude that de Broglie–Bohm causal quantum mechanics is incorrect. Thus, it is remarkable that LRM allows one to realize an experiment that conclusively demonstrates that photons do not propagate following the lines of electromagnetic energy flow.

2. EXPERIMENT DESIGN AND RATIONALE

The interference experiments described in this work were performed using a leakage radiation microscope [1–4] for both exciting two SPP beams in a glass-metal sample and observing their propagation. Figure 1 shows a top view photograph of the surface of a fabricated sample. Samples investigated here were patterned on a glass substrate. A 50 nm thick gold layer was initially deposited on top of a 1 nm thick chromium adhesion layer. The gold layer was covered with poly(methyl methacrylate) (PMMA) as the resist for the electron-beam (e-beam) patterning. A pattern, forming a corner of a square (∟ shape), was defined onto the PMMA layer by e-beam lithography. After developing the PMMA, a second 50 nm thick layer of gold was deposited on the top of the PMMA layer. A final liftoff step produced the desired pattern with a ∟ shape. Each side of the ∟ pattern shown in Fig. 1 consists of a 100 μm long double-stripe structure with a total width of $\sim$1 μm. Each stripe corresponds to a gold ridge with a width of 200 nm. As sketched in Fig. 1, the patterned ∟-shape structure was used to launch two SPP beams perpendicular to each other on the 50 nm thick gold film. The excitation source was provided by a 10 mW He–Ne laser which intensity was equally divided by a cube beam splitter. The two beams were deflected toward a low numerical aperture (NA) (NA=0.65, 40×) microscope objective lens with slightly different angles. As sketched in Fig. 1, the lens focused the beams into spots of diameter $\sim$5 μm on each side of the ∟ pattern. This procedure was used to launch SPP beams that propagate through the gold–air interface perpendicularly to the sides of the ∟ pattern [1,2].

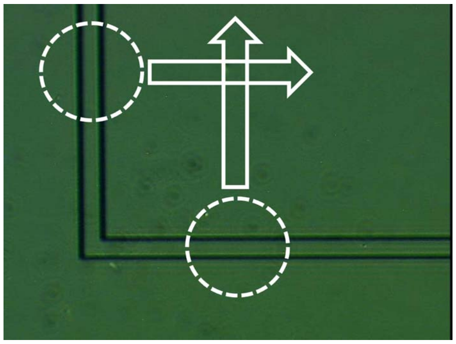

Fig. 1. (Color online) Top view photograph of the surface of a fabricated sample. The dashed circles illustrate the position of the focused spots. Added arrows indicate the direction of propagation of the launched SPP beams.

Launched SPP beams freely propagate on the metal–air interface and radiation leaked to the sample substrate is collected by the microscope 100× immersion oil objective lens (NA=1.3). A charge-coupled device (CCD) camera captures the image of the sample surface emission after being partially reflected by a beam splitter internal to the microscope body. A second CCD camera captures the image formed in the back focal plane (BFP) of the immersion oil objective.

When a SPP beam is launched in the sample surface, (1) SPP-coupled radiation leaks to the sample substrate from any point of the sample metal–air interface that the SPP beam passes through and (2) SPP-coupled radiation leaks to the sample substrate in the direction of propagation of the SPP beam [1–6]. These two principles determine the image formation in LRM. Propagation of SPP and leakage radiation are linear phenomena; thus, when several SPP beams are simultaneously launched the two principles mentioned above apply to each beam separately. Based on these two principles, Fig. 2(a) illustrates the anticipated sample surface emission image when the SPP beams are simultaneously launched by the two focused spots sketched in Fig. 1. SPP-coupled radiation leaks to the sample substrate from any point of the sample metal-air interface that a SPP beam passes through. Consequently, a bright cross corresponding to the propagation of two SPP beams should be observed [1,3]. The bright cross in Fig. 2(a) is the image of the propagation of two SPP beams. One SPP beam is launched by the spot focused on the vertical arm of the ∟ pattern (see Fig. 1) and propagates from left to right in Fig. 2(a). The second SPP beam is launched by the spot focused on the horizontal arm of the ∟ pattern (see Fig. 1) and propagates from bottom to top in Fig. 2(a). In addition, as shown in Fig. 2(a), interference fringes should be clearly observed in the crossing region of the two SPP beams [4]. Besides the image of the sample surface emission, LRM also permits one to obtain the image formed at the BFP of the microscope high NA objective lens. The BFP image corresponds to the Fourier plane with respect to the sample surface emission and thus to a map of the two-dimensional momentum distribution of the SPP propagation in the gold–air interface of the sample [1–6]. Consequently, in the absence of diffraction effects, the leakage radiation leaks to the sample substrate in the direction of propagation of the SPP excitation. Figure 2(b) shows the schematic illustration of the expected BFP image corresponding to the image of the sample surface emission shown in Fig. 2(a). The trace at the right extreme in Fig. 2(b) corresponds to the SPP beam propagating from left to right in Fig. 2(a) [1,3]. The trace at the top extreme in Fig. 2(b) corresponds to the SPP beam propagating from bottom to top in Fig. 2(a). The presence or absence of the additional trace shown in Fig. 2(b) in between the right and top traces is the more important feature in the BFP image. As it will be discussed below, the additional trace should be present if photons propagate following the classical lines of electromagnetic energy flow, but a quantum description of light predicts the absence of the additional trace. In correspondence with the quantum description of light, experimental results reported in this work unequivocally establish that no trace in addition to the right and top traces appears on the BFP image.

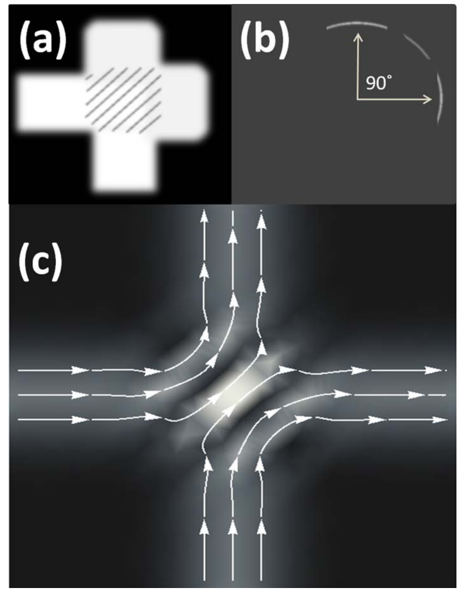

Fig. 2. (Color online) Schematic of the expected (a) sample surface emission and (b) BFP images in the described experiments. (c) Calculated lines of energy flux in the crossing area. Arrows in (b) and (c) indicate the direction of propagation of the electromagnetic energy.

Figure 2(c) shows the lines of electromagnetic energy flow in the beams' crossing region. These lines, tangent to the Poynting vector at every point [7,8], were calculated by solving the Maxwell's equations using standard numerical methods. As shown in Fig. 2(c), the direction of the Poynting vector forms an angle of ~45° with the horizontal in a considerable fraction of the crossing region area. That is, the lines of electromagnetic energy flow are parallel to the interference maxima formed where the beams cross each other. SPP-coupled radiation leaks to the sample substrate in the direction of propagation of the SPP excitation; thus, with the microscope focused on the crossing region, if photons in the SPP beams propagate following the lines of electromagnetic energy flow [9–12], it should be expected that a significant fraction of the leakage radiation leaks to the sample substrate in an intermediate direction with respect to the directions of the

SPP beams. This would result in the observation of an additional trace in the BFP image as shown in the top-right corner of Fig. 2(b).

A quantum description of the interference of the SPP beams asserts that some photons traversing the crossing region eventually leak to the glass substrate. Each leaked photon ends producing a photodetection event ("click") at the CCD camera used to record the BFP image in the microscope. When only one SPP beam is launched, each photon in a SPP beam propagating from left to right through the gold–air interface of the sample is in the Dirac's translational state $|h\rangle$, while each photon in a SPP beam propagating from bottom to top is in the state $|v\rangle$ [17]. The probability amplitude that a photon in the state $|h\rangle$ produces a click at the top extreme of the CCD camera screen is zero. It is also zero the probability amplitude that a photon in the state $|v\rangle$ produces a click at the right extreme of the CCD camera screen. However, when the two SPP beams are simultaneously launched, each photon traversing the beams' crossing region is in the state $|I\rangle = \frac{1}{\sqrt{2}}[|h\rangle + |v\rangle]$ [18]. Following Feynman's quantum rules for interference [18], the probability amplitude that a photon in the state $|I\rangle$ produces a click at a given pixel of the CCD camera screen is equal to the sum (properly normalized to 1) of the independent probability amplitudes corresponding to the states $|h\rangle$ and $|v\rangle$. Thus, half of the photons should end at the right extreme of the CCD camera screen, and the other half should end at its top extreme. This produces the traces shown at the right and top extremes of Fig. 2(b). Consequently, a quantum description predicts that the additional trace in the BFP image, shown in the top-right corner of Fig. 2(b), should not be observed.

In summary, this work describes SPP interference experiments using a leakage radiation microscope for excitation of two perpendiculars SPP beams in the gold–air interface of the fabricated samples, collection of the leaked radiation, and image formation. The goal of the experiments is to find out whether photons propagate following the classical lines of electromagnetic energy flow. In a conclusive experiment, as shown in Fig. 2(a), the launched SPP beams should be observed in the surface emission image. Moreover, an interference pattern in the region where the SPP beams cross each other should be observed. This is important because the calculated lines of energy flow have the shape shown in Fig. 2(c) only if the interference pattern is formed, i.e., if a coherent superposition of the SPP beams occurs. The presence of an interference pattern in the surface emission image formed in the screen of the corresponding CCD camera means that the SPP beams coherently superpose each other in the sample's metal–air interface. Once this has been established, the absence in the BFP image of a trace forming an angle of $\sim 45°$ with the direction of propagation of the SPP beams [see Fig. 2(b)] is enough to demonstrate that photons do not propagate following the classical lines of electromagnetic energy flow. It is worth noting that this is a negative demonstration. If such a trace were observed, it would suggest, not demonstrate, that photons propagate following the classical lines of electromagnetic energy flow. This is because it is not possible to observe the trajectory of the photons in the described experiments. The surface emission image [Fig. 2(a)] tells us which points photons passed through in the sample metal–air interface, but there is no information in Fig. 2(a) about the direction of the photons. The BFP image [Fig. 2(b)] tells us the directions of propagation of the photons in the metal–air interface, but there is no information in Fig. 2(b) about where photons leak to the sample substrate. Nevertheless, a result where no trace (forming a 45° angle with the direction of propagation of the SPP beams) appears in the BFP image means that there are no photons propagating in that direction in any place in the observed metal–air interface. This contradicts the classical electrodynamics prediction that the electromagnetic energy (photons) should propagate parallel to the interference fringes formed in the region where the SPP beams cross each other.

3. EXPERIMENTAL RESULTS AND DISCUSSION

Figure 3(a) shows the image of the sample surface emission obtained with LRM. In excellent agreement with Fig. 2(a), two SPP beams are clearly observed. Furthermore, interference fringes with good visibility are present in the region where the beams cross each other. Figure 3(b) shows the corresponding BFP image. The two well-defined bright traces at the right and top extremes of Fig. 3(b) correspond to the SPP beams propagating from left to right and from bottom to top [see Fig. 3(a)], respectively. More significantly, no additional trace with a maximum intensity in between the two traces is observed in Fig. 3(b). These experimental results demonstrate that photons do not propagate following the lines of energy flow. Consequently, the lines of electromagnetic energy flow calculated using the classical theory of electrodynamics should be interpreted as indicating the direction of propagation of the average electromagnetic energy. Individual photons conserve their momenta in the crossing region where interference occurs. However, the average momentum of the light at any place points in the direction tangent to the lines of energy flow.

In order to corroborate that photons passing through the beams' crossing region conserve the direction of the input beams, an additional magnifying lens was introduced in the optical path of the light in the microscope. The lens was placed before the beam splitter that sends light to both microscope cameras. In this way both images are formed by photons that leaked from the same region of the sample surface. Figure 4(a) shows a magnified view

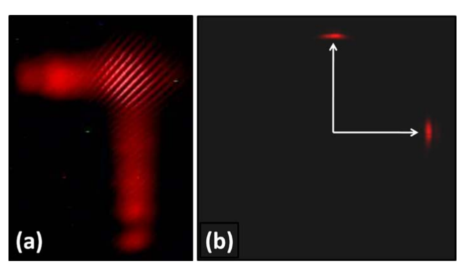

Fig. 3. (Color online) (a) Sample surface emission and (b) BFP images obtained with a leakage radiation microscope. Arrows were added to guide the eyes.

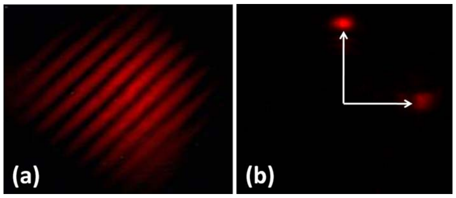

Fig. 4. (Color online) Magnified view of (a) sample surface emission and (b) BFP images corresponding to the beams' crossing region. Arrows were added to guide the eyes.

of the crossing area. Well-defined interference fringes forming an angle of 45° with the beams fill the complete image. This means that (1) the SPP beams coherently superpose each other in the sample metal–air interface and (2) all photons arriving to both cameras come from the region in the metal–air interface where the SPP beams cross each other. Nevertheless, as shown in Fig. 4(b), only two traces in the directions of propagation of the beams are observed in the BFP image. This conclusively demonstrates that photons passing through the beams' crossing region leaks to the sample substrate in the direction of the beams. Consequently, photons conserve their directions of propagation in the crossing region where interference fringes are observed. That is, photons do not propagate in the beams' crossing region following the classical lines of energy flow. It is worth noting that the surface emission image was only used to be sure that the SPP beams coherently superpose each other in the sample's metal–air interface. Once this was established, one could have removed the CCD camera used to obtain the sample surface emission image without altering the propagation of the SPP beams in the sample's metal–air interface. Moreover, one could have redirected all photons to the CCD camera used to obtain the BFP image (for instance, by substituting the beam splitter internal to the microscope body with a mirror) without altering the propagation of the SPP beams in the sample's metal–air interface or the BFP image shown in Fig. 4(b). Thus, the experiments presented in this work conclusively demonstrated that photons passed through the beams' crossing region following the original directions of the launched SPP beams. This brings the attention to another counterintuitive manifestation of Heisenberg's uncertainty principle [18]. It looks like somehow photons should pass through the dark fringes defined in the beams' crossing area by the interference minima [see Fig. 4(a)]. A photon propagation paradox then arises as to how a photon can propagate across a region where it is never observed [11]. When the interference pattern is formed in the metal–air interface, photons propagate through the beams' crossing region in two directions perpendicular to each other with a momentum of magnitude given by de Broglie's formula $p \sim h/\lambda$ [18]; thus, the uncertainty in the value of the component of the photon momentum in the direction perpendicular to the interference fringes is equal to

$$\Delta p \sim \sqrt{2}\frac{h}{\lambda}, \tag{1}$$

where h is the Plank's constant and λ is the SPP wavelength. While a photon is passing from one interference maxima to the next one, the uncertainty in the determination of the photon position in the direction perpendicular to the fringes (Δx) is determined by the distance between consecutive interference maxima. That is, Δx is given by the following expression [19]:

$$\Delta x \sim \frac{\sqrt{2}}{2}\lambda. \tag{2}$$

From expressions (1) and (2) it follows that $\Delta x \Delta p \sim h$. That is, the separation between consecutive interference maxima is in correspondence with quantum mechanics Heisenberg's uncertainty principle.

4. CONCLUSIONS

A leakage radiation microscope was used for launching two perpendicular SPP beams in the gold–air interface of the fabricated samples, collection of the leaked radiation, and image formation. To the best of the author's knowledge, in this work, direct experimental evidence that conclusively demonstrates that photons do not propagate following the classical lines of electromagnetic energy flow was presented for the first time. The experimental results are in agreement with widespread quantum descriptions of light. It is worth noting that the experiments presented in this work permit one to arrive to this conclusion because LRM allows for the observation of SPP propagation without disturbing the two-dimensional interference pattern formed at the region where the beams cross each other.

ACKNOWLEDGMENTS

This work was partially supported by the National Science Foundation (NSF) CAREER award (ECCS-0954490) and by the J. F. Maddox Foundation. The author recognizes the help of Moses Marchante and Jacob Ajimo in the conducting of the experiments, Ananth Krishnan in the fabrication of the samples, and the fruitful discussions with Ayrton Bernussi about the interpretation of the experimental results.

REFERENCES

1. A. Drezet, A. Hohenau, D. Koller, A. Stepanov, H. Ditlbacher, B. Steinberger, F. R. Aussenegg, A. Leitner, and J. R. Krenn, "Leakage radiation microscopy of surface plasmon polaritons," Mater. Sci. Eng., B **149**, 220–229 (2008).
2. J.-Y. Laluet, A. Drezet, C. Genet, and T. W. Ebbesen, "Generation of surface plasmons at single subwavelength slits: from slit to ridge plasmon," New J. Phys. **10**, 105014 (2008).
3. S. Massenot, J. Grandidier, A. Bouhelier, G. Colas des Francs, L. Markey, J.-C. Weeber, A. Dereux, J. Renger, M. U. Gonzàlez, and R. Quidant, "Polymer-metal waveguides characterization by Fourier plane leakage radiation microscopy," Appl. Phys. Lett. **91**, 243102 (2007).
4. A. Drezet, A. Hohenau, A. L. Stepanov, H. Ditlbacher, B. Steinberger, N. Galler, F. R. Aussenegg, A. Leitner, and J. R. Krenn, "How to erase surface plasmon fringes," Appl. Phys. Lett. **89**, 091117 (2006).
5. S. P. Frisbie, C. Chesnutt, M. E. Holtz, A. Krishnan, L. Grave de Peralta, and A. A. Bernussi, "Image formation in wide-field microscopes based on leakage of surface plasmon-coupled fluorescence," IEEE Photonics Journal **1**, 153–162 (2009).
6. A. Krishnan, S. P. Frisbie, L. Grave de Peralta, and A. A.

Bernussi, "Plasmon stimulated emission in arrays of bimetallic structures coated with dye-doped dielectric," Appl. Phys. Lett. **96**, 111104 (2010).
7. J. D. Jackson, *Classical Electrodynamics* (Wiley, 1962).
8. M. Born and E. Wolf, *Principles of Optics* (Pergamon, 1975).
9. R. D. Prosser, "The interpretation of diffraction and interference in terms of energy flow," Int. J. Theor. Phys. **15**, 169–180 (1976).
10. R. D. Prosser, "Quantum theory and the nature of interference," Int. J. Theor. Phys. **15**, 181–193 (1976).
11. J. P. Wesley, "A resolution of the classical wave-particle problem," Found. Phys. **14**, 155–170 (1984).
12. A. S. Sanz, M. Davidović, M. Božić, and S. Miret-Artés, "Understanding interference experiments with polarized light through photon trajectories," Ann. Phys. (N.Y.) **325**, 763–784 (2010).
13. D. Bohm, "A suggested interpretation of the quantum theory in terms of hidden variables I," Phys. Rev. **85**, 166–179 (1952).
14. D. Bohm, "A suggested interpretation of the quantum theory in terms of hidden variables II," Phys. Rev. **85**, 180–193 (1952).
15. C. Philippidis, D. Bohm, and R. D. Kaye, "The Aharonov–Bohm effect and the quantum potential," Nuovo Cimento **71B**, 75–88 (1982).
16. P. R. Holland, *The Quantum Theory of Motion: An Account of the Broglie–Bohm Causal Interpretation of Quantum Mechanics* (Cambridge Univ. Press, 1993).
17. P. A. M. Dirac, *The Principles of Quantum Mechanics*, 4th ed. (Clarendon, 1958).
18. R. P. Feynman, R. B. Leighton, and M. Sands, *The Feynman Lectures on Physics* (Addison-Wesley, 1965), Vol. II.
19. F. L. Pedrotti, L. S. Pedrotti, and L. M. Pedrotti, *Introduction to Optics*, 3rd ed. (Pearson Prentice Hall, 2007).